

A Novel Approach to Overcome Cisplatin Resistance in Ovarian Cancer: Revealing the Synergistic Potential of Quercetin-Loaded Solid Lipid Nanoparticles

Masoumeh Shamsi¹, Hossien Babaahmadi-Rezaei²,
Azam Khedri¹, Mahdi Hatami², Mojtaba Rashidi^{1,2*}

¹Cellular and Molecular Research Center, Medical Basic Sciences Research Institute, Ahvaz Jundishapur University of Medical Sciences, Ahvaz, Iran; ²Department of Clinical Biochemistry, Faculty of Medicine, Ahvaz Jundishapur University of Medical Sciences, Ahvaz, Iran

ABSTRACT

OPEN ACCESS

Article type: Research Article
Received: December 10, 2024
Revised: December 27, 2024
Accepted: December 31, 2024
Published online: January 2, 2025

How to cite:

Shamsi M, Babaahmadi-Rezaei H, Khedri A, Hatami M, Rashidi M. A Novel Approach to Overcome Cisplatin Resistance in Ovarian Cancer: Revealing the Synergistic Potential of Quercetin-Loaded Solid Lipid Nanoparticles. *Iran. Biomed. J.* 2025; 29(1&2): 20-35.



This article is licensed under a Creative Commons Attribution-NonDerivatives 4.0 International License.

Background: Ovarian cancer remains the leading cause of mortality among gynecological cancers, mainly because of resistance to platinum-based chemotherapy, particularly cisplatin. This study investigated the potential of QU-loaded SLNs to address cisplatin resistance in OC cells.

Methods: The efficacy of QU-SLN was assessed in vitro on the cisplatin-resistant SK-OV-3 and cisplatin-sensitive A2780s human OC cell lines. Various assays, including cytotoxicity, cell viability, clonogenicity, flow cytometry, quantitative RT-PCR, and wound healing assays, evaluated the combined effects of QU and QU-SLN with cisplatin on cell viability, apoptosis, gene expression levels related to cisplatin resistance, and cell migration.

Results: Combining QU-SLN with cisplatin resulted in significantly reduced cell viability and colony formation, accompanied by increased apoptotic rates compared to each treatment alone. Moreover, there was a notable reduction in the expression level of genes associated with cisplatin resistance, particularly *ABCG2*, *MT-2A*, *GST-pi*, and *XIAP*, in the combined treatment. Wound healing assays indicated that the QU-SLN and cisplatin combination severely impaired OC cell motility compared to cisplatin monotherapy.

Conclusion: QU-SLN and cisplatin combination enhances the therapeutic response in cisplatin-resistant OC cells. By reducing cell proliferation, promoting apoptosis, and downregulating drug resistance genes, QU-SLN might present a promising strategy to improve treatment outcomes for OC patients resistant to cisplatin. **DOI: 10.61186/ibj.4543**

Keywords: Nanoparticles, Ovarian neoplasms, Quercetin

Corresponding Author: Mojtaba Rashidi

Cellular and Molecular Research Center, Medical Basic Sciences Research Institute, Ahvaz Jundishapur University of Medical Sciences, Ahvaz, Iran; Department of Clinical Biochemistry, Faculty of Medicine, Ahvaz Jundishapur University of Medical Sciences, Ahvaz, Iran; Tel.: (+98-916)6131031; E-mail: ms_rashidi60@yahoo.com; ORCID ID: 0000-0003-43111-6137

List of Abbreviations:

OC: ovarian cancer; **QU:** quercetin; **SLN:** solid lipid nanoparticle; **RT-PCR:** real-time polymerase chain reaction; **GST:** glutathione S-transferase; **ABC:** ATP-binding cassette; **XIAP:** X-linked inhibitor of apoptosis protein; **GSH:** glutathione; **FTIR:** Fourier transform infrared spectroscopy; **TEM:** transmission electron microscopy; **PDI:** polydispersity index; **EE:** encapsulation efficiency; **PBS:** phosphate-buffered saline; **DLS:** dynamic light scattering

INTRODUCTION

Ovarian cancer is the second most common gynecological cancer and the fifth leading cause of cancer-related deaths among women globally. Mortality from OC is projected to triple by 2040, although breast cancer is more common. The three main categories of OC are stromal tumors, germ cell tumors, and epithelial carcinoma, accounting for 85–90% of occurrences. Epithelial carcinoma is divided into different subtypes, including serous and endometrioid tumors. Pregnancy and using oral contraceptives serve as protective factors; however, advanced age, family history, and reproductive variables are risk factors^[1-4]. Cytoreductive surgery and platinum-based chemotherapy are the standard treatments, with cisplatin being a crucial medication^[3,5]. Two resistance ways to cisplatin arise from reduced drug absorption and improved detoxification by enzymes, such as GST-pi, which prevents apoptosis and encourages drug efflux^[6]. Treatment is complicated by multidrug resistance, primarily through ATP-binding cassette transporters such as ABCG2^[7], and XIAP, which interfere with apoptotic pathways, further contributing to chemoresistance in OC^[8].

Recent therapeutic approaches have investigated the synergy between bioflavonoids, such as QU, and traditional chemotherapeutics to improve tumor cell targeting. In recent years, research on SLNs as a drug delivery system has gained significant importance due to their potential to enhance the bioavailability of poorly water-soluble drugs. QU, a flavonoid with recognized therapeutic properties, is limited in clinical use because of its low water solubility and poor bioavailability.

Encapsulating QU into SLNs has emerged as a promising strategy to overcome these limitations. The solubility and bioavailability of QU are improved by nanoformulation, which also protects it from chemical and enzymatic breakdown for long-lasting effects on the body^[9,10]. Additionally, SLNs can be tailored for specificity toward particular cell types or tissues, including cancer cells, facilitating targeted delivery and reducing off-target side effects. The controlled release properties of SLNs help maintain therapeutic concentrations of QU in cells for an extended period, thereby optimizing its cytotoxic effects^[11]. Furthermore, encapsulation in SLNs may assist in circumventing drug resistance mechanisms that often diminish the efficacy of chemotherapeutic agents, such as cisplatin, by altering the pharmacokinetics and biodistribution of QU. These properties underscore the rationale for selecting SLNs as drug carriers for QU, based on recent studies highlighting the potential for improved therapeutic outcomes in various clinical settings^[12,13].

In this work, we decided to initially test the efficacy of QU nanoparticles and subsequently analyze their effect and mode of action concerning the reduction of cisplatin-related drug resistance in OC cells. The study aimed to understand the effects of QU-SLN on the sensitivity of OC cells to low concentrations of cisplatin.

MATERIALS AND METHODS

Preparation of QU-SLN

To prepare QU-SLN, 100 mg of QU (Sigma Aldrich St. Louis, MO, USA) was mixed with 4.75 g of Compritol 888 ATO (Glyceryl Dibehenate, Gattefossé, France) at 75 °C. Subsequently, oleic acid (0.25 g) and lecithin (0.5 g) were dissolved in deionized water preheated to 80 °C. This solution was then combined with the initial QU mixture and emulsified using an Elmasonic S60H Sonicator (Global Industrial, USA) for five minutes. The resulting solution was mixed with 4 mL of 1% polyvinyl alcohol at 4 °C, leading to a nanoemulsion. This emulsion was then homogenized using a Heidolph homogenizer (Germany) operating at 1,323 ×g. The final product was subjected to two rounds of centrifugation at 5290 ×g for 25 min at 5 °C. The resulting QU-SLNs were stored in airtight containers and refrigerated for further use.

Fourier transform infrared spectroscopy

To evaluate the intermolecular interactions within the SLN following the encapsulation of QU, FTIR spectra were captured using a VERTEX 70v FTIR spectrometer (Bruker, USA). Pellets were formed by compressing blank-SLN, QU-SLN, and pure QU with potassium bromide under a 200 kg/cm² pressure. The spectra resulting from this process were recorded at a resolution of 4 cm⁻¹, within the spectral range of 400–4000 cm⁻¹.

Transmission electron microscopy

The structure of the SLNs was examined using TEM. A droplet of the nanoparticle solution was placed on a copper grid coated with carbon, forming a thin film. Any surplus liquid was absorbed using filter paper, and the grid was allowed to air dry at ambient temperature for five minutes. The morphology of the SLNs was then scrutinized using a ZEISS LEO 906 E TEM (Germany).

Zeta potential and particle size determination

The mean particle size, PDI, and zeta potential of the QU-SLNs were determined using a Malvern Zetasizer Nanosizer (England).

Measurement of EE

The percentage of entrapment efficiency (EE of QU

was determined using ultraviolet-visible spectrophotometry based on a previously constructed and validated calibration curve of QU in methanol (Fig. S1), at a wavelength (λ) of 256 nm (UV 1700, Shimadzu, Kyoto, Japan). After the separation of SLNs containing QU (centrifuged at 1500 \times g for 7 minutes), the free QU was measured. The EE was computed using the following formula: $EE (\%) = [(Di-Df)/Di] \times 100$, where Di denotes the initial total quantity of the drug, and Df signifies the quantity of the drug that remains unencapsulated. To determine the drug loading, 100 mg of the formulation was extracted using absolute methanol. The extracted QU was then diluted to a final volume of 10 mL, and the content of QU in the solution was analyzed using spectrophotometry at a wavelength of 256. The formula used was as follows: $DL (\%) = [\text{drug loaded/lipid weight}] \times 100^{[14]}$.

Storage stability of QU-SLNs

The storage stability of QU-SLNs was evaluated at 4 °C for 10 days after manufacturing. The absorbance at 256 nm was measured to calculate the remaining amount of QU in the formulations. The retention index was then determined using the following formula: retention index (%) = $C_R/C_i \times 100$, where C_i and C_R indicate the initial and remaining concentrations of the QU in the SLN, respectively^[15]. The calibration curve was used to determine the sample concentration. In addition, the formulations were stored at 4 °C for 3 months.

In vitro drug release study

The release of QU from the QU-SLN was evaluated at 37 °C using a dialysis bag (Sigma-Aldrich) technique with a molecular weight cut-off of 12,000 Da^[24]. PBS with a pH of 7.42 was used as the receptor phase for the release of free QU from the nanoparticle. Over 72 hours, samples were collected at pre-established intervals. The QU content in these samples was then measured at 256 nm using an Ultrospec 3000 spectrophotometer (Amersham Pharmacia Biotech, USA).

Cell culture

The A2780s and SK-OV-3/DDP OC cell lines, sourced from the Cell Bank of the Pasteur Institute of Iran (Tehran), were cultured in the medium of RPMI 1640, enriched with 10% heat-inactivated fetal bovine serum and 100 U/mL of penicillin/streptomycin (Sigma-Aldrich). The cultures were kept at a temperature of 37 °C in a 5 % CO₂ incubator.

MTT assay

The MTT assay evaluated the inhibitory effects of cisplatin, QU, QU-SLN, and their combinations on the viability of sensitive (A2780s) and resistant (SK-OV-

3/DDP) human OC cells. After seeding the cells (1.0×10^4 cells/well) into 96-well plates, varying concentrations of cisplatin (0.001-25 μ M)^[27], QU (5 - 240 μ mol/L), and QU-SLN (5-80 μ mol/L) were administered to the cells for 24 and 48 hours. Control cells were given an equivalent amount of RPMI-1640 medium. Following the addition of MTT (20 μ L; 5 mg/mL) to each well, the mixture was incubated in darkness at 37 °C for 4 hours. The supernatant from each well was then removed, and 100 μ L of DMSO was added to each well. After shaking the plates on a rotator for 15 minutes, the absorbance was read at 570 nm using a microplate reader (Winooski, USA). The effect of combination treatment was assessed by combining the IC₅₀ value of QU-SLN with the lowest concentration (0.001 μ M) of cisplatin. We assessed the viability of the OC cells in various groups including SK-OV-3/DDP and A2780s cells: (A) control, (B) blank-SLN, (C) cisplatin (0.001 μ M), (D) QU + cisplatin combination, (E) QU-free, (F) QU-SLN + cisplatin combination, and (G) QU-SLN. To this end, cells (1×10^4 cells/mL) were plated and treated with cisplatin, QU, Q-SLN, and a combination treatment (pre-treatment with both QU and QU-SLN for 12 hours, followed by cisplatin). Untreated cells served as controls.

Colony formation assay

Colony formation assay was conducted to evaluate the growth inhibition effect of cisplatin (0.001 μ M), QU, QU-SLN, and their combined treatment (pre-treatment with QU and QU-SLN for 12 h, followed by cisplatin) on OC cells. A2780s and SK-OV-3/DDP cells were seeded at a density of 5,000 cells per well in 2 mL of complete growth media in a six-well plate and were allowed to attach for 24 hours. After attachment, fresh RPMI 1640 and cisplatin (0.001 μ M) were added. Each well received 35.5 μ M of QU and 36.6 μ M of QU-SLN, individually and combined treatment (pre-treatment with QU and QU-SLN for 12 hours, followed by 0.001 μ M of cisplatin). After media refreshment, the cells were placed in a 5% CO₂ humidified chamber at 37 °C for 7 days. Next, the colonies were fixed in a 1:7 (v/v) acetic acid/methanol solution at room temperature for five minutes. The cells were then washed three times with PBS. The colonies were stained using a 0.5% crystal violet solution at room temperature for five minutes, followed by three additional washes with PBS. Then, photographs of the colonies were taken and analyzed using ImageJ software (National Institutes of Health, Bethesda, USA).

Flow cytometry

The Annexin V-FITC/PI Apoptosis Detection Kit (MBR, Zist Exir Teb, Iran) was utilized to analyze cell

apoptosis as per the manufacturer's guidelines. In brief, A2780s and SK-OV-3/DDP cells were seeded at a density of 3.5×10^5 cells/well in six-well plates. Afterwards, each cell was individually exposed to 0.001 μM of cisplatin, with 35.5 μM and 36.6 μM of QU and QU-SLN alone and a combined treatment (pre-treatment with QU and QU-SLN for 12 hours, followed by 0.001 μM cisplatin). The cells were allowed to adhere in a humidified atmosphere containing 5% CO_2 at 37 °C overnight. Following the treatment, the growth media were discarded, the cells were detached from the well, and washed twice with PBS. The cell pellets were then re-suspended in 350 μL of binding buffer. The cell suspension was stained using 3 μL of Annexin V-FITC in the dark at room temperature for 15 minutes and then 2 μL of propidium iodide for 5 minutes. Finally, 10,000 events were evaluated using the BD FACSCalibur Flow Cytometry System (BD Biosciences, USA).

Real-time polymerase chain reaction

The total RNA isolation kit (Yekta Tajhiz Azma, Iran) was utilized to extract high-quality RNA from 10^6 cells, and then the isolated RNA was preserved in 50 μL of DEPC-treated water at -70 °C. The integrity and purity of the RNA were verified through agarose gel electrophoresis. Reverse transcription was conducted in a 20 μL reaction mixture using the cDNA synthesis kit, following the manufacturer's instructions. Subsequently, PCR was performed as follows: initial denaturation at 95 °C for 15 minutes, followed by 40 amplification cycles (15 seconds at 95 °C and 1 minute at 60 °C). *GAPDH* was employed as the housekeeping gene, and the $2^{-\Delta\Delta C_t}$ method was used for fold change calculation. The primer sequences are listed in [Table S1](#).

Wound healing assay

Upon seeding the 2×10^5 cells in each well of a six-well plate and achieving 90% confluency, a horizontal scratch was created using a 100 μL pipette tip. The wells were then washed twice with PBS. Following treatment with cisplatin, QU, and QU-SLN and their combinations (pre-treatment with QU and QU-SLN for 12 h, followed by cisplatin) for 24 and 48 hours, photographs were taken at the 0, 24, and 48-hour marks, and the images were subsequently analyzed using ImageJ software (National Institutes of Health, USA).

Statistical analysis

Each experiment was conducted in triplicate presented as mean \pm SD. Statistical analysis was performed using GraphPad Prism 8. One-way ANOVA followed by

Tukey's post hoc test was used for multiple comparisons, with $p < 0.05$ considered statistically significant.

RESULTS

FTIR analysis

The FTIR spectral analysis of QU-SLN, revealed several characteristic absorption bands: a broad O-H stretching band (3850-3200 cm^{-1}), C-O stretching vibration (1635 cm^{-1}), C-C stretching vibration (1659 cm^{-1}), C-H bending vibrations (1463 and 1379 cm^{-1}), and two bands attributable to C-O stretching corroborating the molecular interactions between QU and SLNs ([Fig. S2](#)).

Characterization of QU-SLN

TEM images revealed an average nanoparticle diameter of 150 ± 20.5 nm ([Fig. 1A](#)). The surface charge of the QU-SLN nanoparticles, measured as zeta potential, was found to be approximately -27.7 mV, indicative of a negative charge contributing to their colloidal stability and resistance to aggregation ([Fig. S3](#)). The PDI was recorded at 0.50 ± 0.04 , suggesting a uniform particle size distribution. This size is consistent with the average particle diameter of 156 nm obtained through DLS measurements, confirming that most of the QU-SLN particles were smaller than 156 nanometers ([Fig. S4](#)). The concentrations of QU were calculated from the absorbance measurements using appropriate calibration curves. EE was 99.68%, and drug loading was 1.81%, further confirming the successful construction of QU-SLNs. The encapsulation of SLNs significantly improved its stability during storage ([Fig. S5](#)). In the formulation of QU-SLN, lecithin and oleic acid created a stable nanoemulsion as a surfactant, while polyvinyl alcohol at 1% concentration served as a stabilizer, preventing nanoparticle aggregation during homogenization ([Table S2](#)).

Drug release profile

Figure 1B illustrates the differential release kinetics of QU in both solution and encapsulated form (QU-SLN). The QU-SLN formulation exhibited a sustained release profile, extending the release of QU for three days. Within the first 12 hours, QU-SLN released approximately 66% of the encapsulated QU, which incrementally increased to 91% over the 72 hours. In contrast, solution of QU alone exhibited a rapid release, achieving nearly complete release (100%) within five hours.

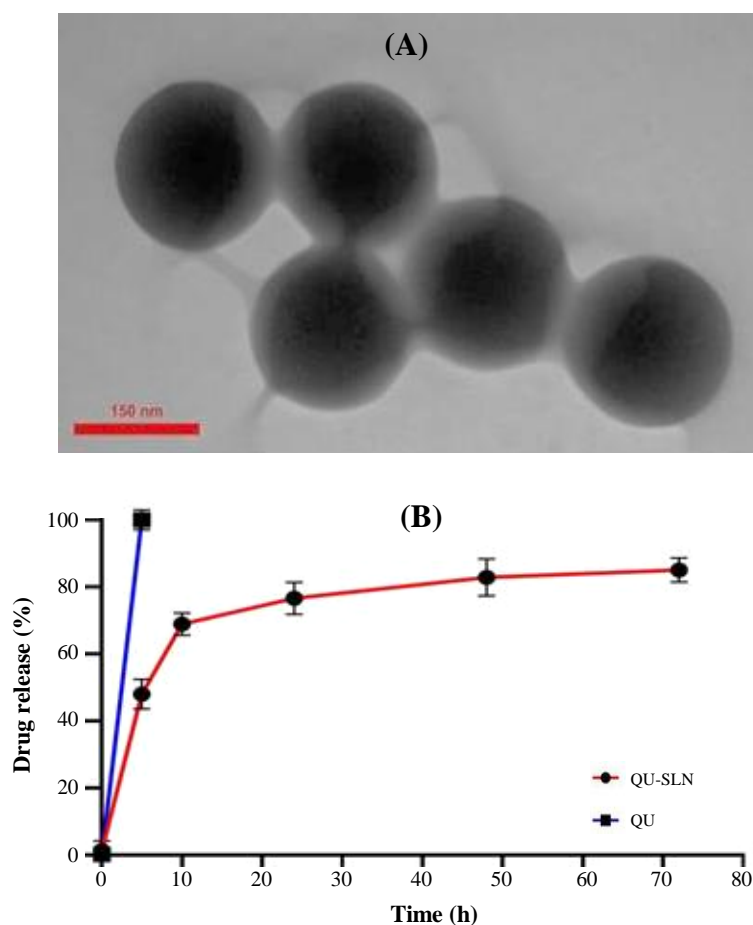


Fig. 1. (A) TEM micrograph of QU-SLN; (B) proportion of QU-SLN released in vitro at different time points.

Cytotoxicity and cell viability

The cytotoxic effect of cisplatin, as a chemotherapy drug, was evaluated on A2780s (cisplatin-sensitive) and SK-OV-3/DDP (cisplatin-resistant) cell lines (Fig. S6A). A dose- and time-dependent growth inhibition was observed with cisplatin treatment over 24 and 48 hours for both QU and QU-SLN (Fig. S6B and S6C, respectively). The IC_{50} values are presented in Table S3. Subsequent investigations focused on the combined effect of cisplatin with QU and QU-SLN on cell viability. Equal concentrations of SLN-blank, QU, and QU-SLN were applied to the cells based on the determined IC_{50} values (35.5 μ M for A2780s and 36.16 μ M for SK-OV-3). A pre-treatment period of 12 hours with either QU or QU-SLN was followed by adding cisplatin at a minimal concentration (0.001 μ M) at which it did not significantly affect the cell viability, independently. Results indicated that SLN-blank alone did not significantly influence cell viability. Notably, combining cisplatin with QU-SLN resulted in a more pronounced inhibition of cell viability in both cell lines

compared to the effects of cisplatin alone and in combination with QU (Fig. 2).

Clonogenic assay

The clonogenic assay was conducted to assess the effects of various treatments on colony formation (Fig. 3A and 3B). In this assay, blank-SLN showed no significant effect on colony formation in both cell lines compared to the control group. The cisplatin group also did not demonstrate a statistically significant decrease compared to the control ($p = 0.1119$). However, A2780s cells treated with the combination of QU + cisplatin at 35.5 μ M showed a significant reduction in colony numbers ($p = 0.0121$). Similarly, those treated with QU-SLN + cisplatin at the same concentration also showed a significant colony formation reduction ($p = 0.0001$). The number of colonies in both treatments were significantly lower than the control group ($p < 0.001$). In the SK-OV-3/DDP cells, the combination of QU + cisplatin at 36.16 μ M resulted in a significant reduction ($p = 0.028$), and QU-SLN + cisplatin at

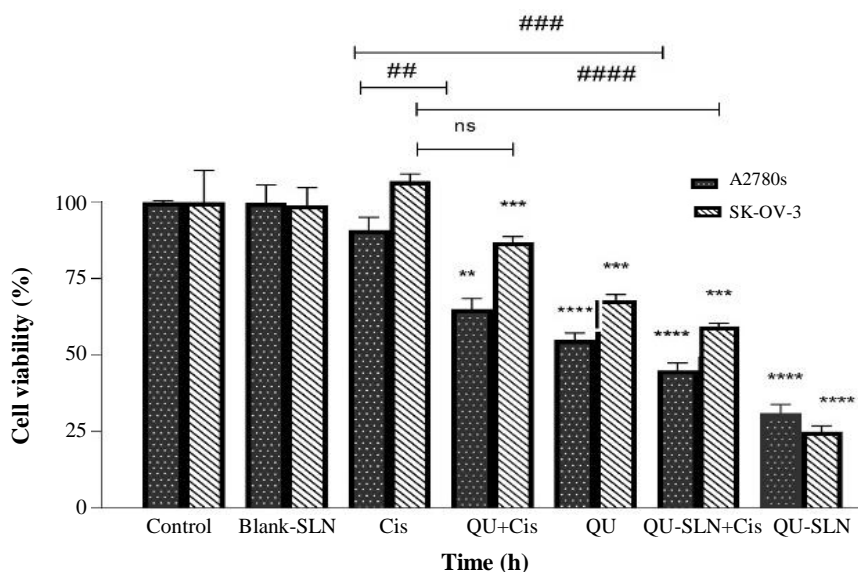


Fig. 2. The viability of A2780s and SK-OV-3/DDP cells assessed using the MTT test after 48 hours of treatment. A2780s and SK-OV-3/DDP cells were treated with 35.5 μM and 36.6 μM of blank SLN, QU, and QU-SLN, respectively. These drugs were selected to observe the pre-treatment effect on both cell types following combination treatment with cisplatin (Cis) at 0.001 μM . The data is presented as mean \pm SD. Statistically significant differences were observed when compared with the control ** $p < 0.01$, *** $p < 0.001$, and **** $p < 0.0001$ and ### $p < 0.01$, #### $p < 0.001$, ***** $p < 0.0001$ when compared to the cisplatin 0.001 μM group. ns: not significant

the same concentration also significantly decreased colony formation ($p = 0.0004$). In both cell lines, the inhibitory effects of the combination groups were significantly greater than those of the cisplatin 0.001 μM treatment groups ($p < 0.001$). Additionally, QU-SLN dramatically reduced the number of colonies compared to QU alone in the sensitive cells, highlighting its potential to overcome resistance in OC (Fig. 3C).

Flow cytometry analysis of cell apoptosis

The current investigation demonstrated that the group treated with QU-SLN plus cisplatin ($p = 0.0001$ and $p < 0.0001$) exhibited significantly higher rates of cell death compared to the QU + cisplatin group ($p = 0.0004$ and $p = 0.0106$) and the cisplatin alone group ($p = 0.859$) in A2780s and SK-OV-3/DDP cells, respectively. Blank SLN did not have any apoptotic effect on the cells. As shown in Figure 4, the QU-SLN + cisplatin group displayed a significantly greater late apoptotic rate (32.48%) than the cisplatin alone group (100%). The early and late apoptosis rates in the QU, cisplatin, and QU-SLN + cisplatin groups were 42.67%, 40.73%, and 71.24%, respectively (Fig. 4). In both A2780s and SK-OV-3/DDP cells, QU-SLN and cisplatin worked synergistically to induce more significant cell death in the sensitive OC cells compared to resistant ones. Overall, the results indicated that QU-SLN and cisplatin could work together to promote cell death in both cell lines.

Quantitative RT-PCR

Quantitative RT-PCR was conducted to investigate the impact of combined treatments on the expression of the genes linked to cisplatin resistance, including ABC-G2, MT-2A, GST-pi, and XIAP. During a 48-hour treatment of cisplatin 0.001 μM alone, the relative expression of the ABC-G2, MT-2A, GST-pi, and XIAP genes significantly increased in both ovarian cells compared to the control group ($p < 0.0001$). These findings explain the phenomenon of cisplatin resistance in OC, wherein cisplatin expression gene chemoresistance may have a major contribution. Furthermore, Blank-SLN had a negligible impact on gene expression, i.e. the levels of ABC-G2, MT-2A, GST-pi, and XIAP expression were downregulated by the combined action of QU-SLN and cisplatin group in comparison with QU + cisplatin and cisplatin alone ($p < 0.0001$; Fig. 5). Comparing QU-SLN + cisplatin to the cisplatin group, a significant high reduction in ABC-G2 gene expression (fold change of 6.865) and a slight reduction in GST-pi expression (fold change of 2.478) was observed in both cell lines (Fig. 5). In addition, the GST-pi, XIAP and ABC-G2 expression levels in SK-OV-3/DDP cells were significantly higher than that of A2780s ($p < 0.0001$). In addition, there was a significant increase in the expression level of MT-2A in both cell lines compared to the cisplatin 0.001 μM group ($p = 0.0063$; Fig. 5).

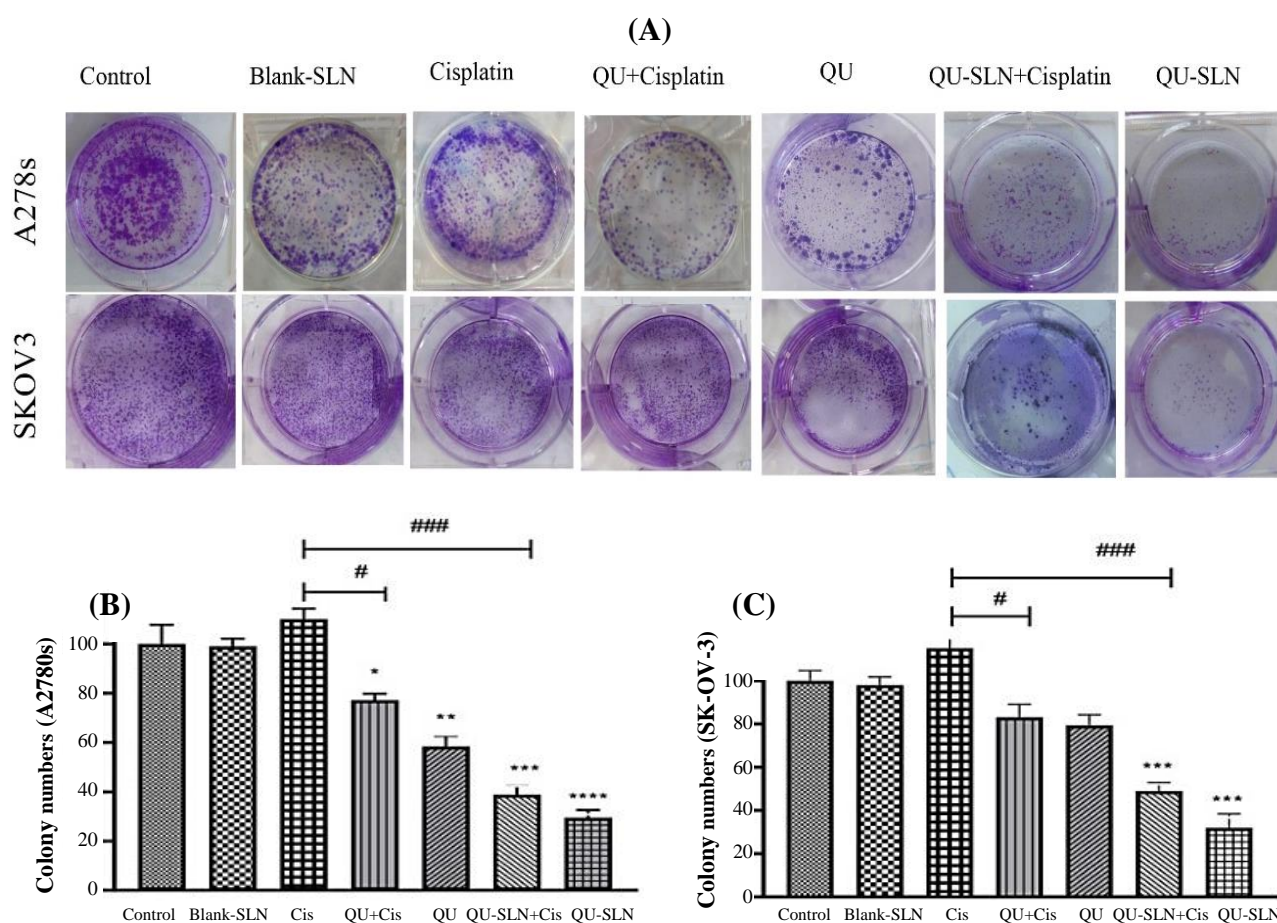


Fig. 3. Colony formation assay conducted on A2780s and SK-OV-3/DDP cell lines. Images of the colonies in both cell lines were captured after 48 hours of treatment with various agents: blank-SLN, cisplatin, QU + cisplatin (Cis), QU, QU-SLN + cisplatin, and QU-SLN. These images were taken for the treated and untreated groups (A). ImageJ software was employed to calculate the mean colony number \pm SD for both the treated and untreated groups (B and C). Statistically significant differences were observed when compared with the cisplatin 0.001 μ M group ($*p < 0.05$, $###p < 0.001$) and the control group ($*p < 0.05$, $**p < 0.01$, $***p < 0.001$, $****p < 0.0001$).

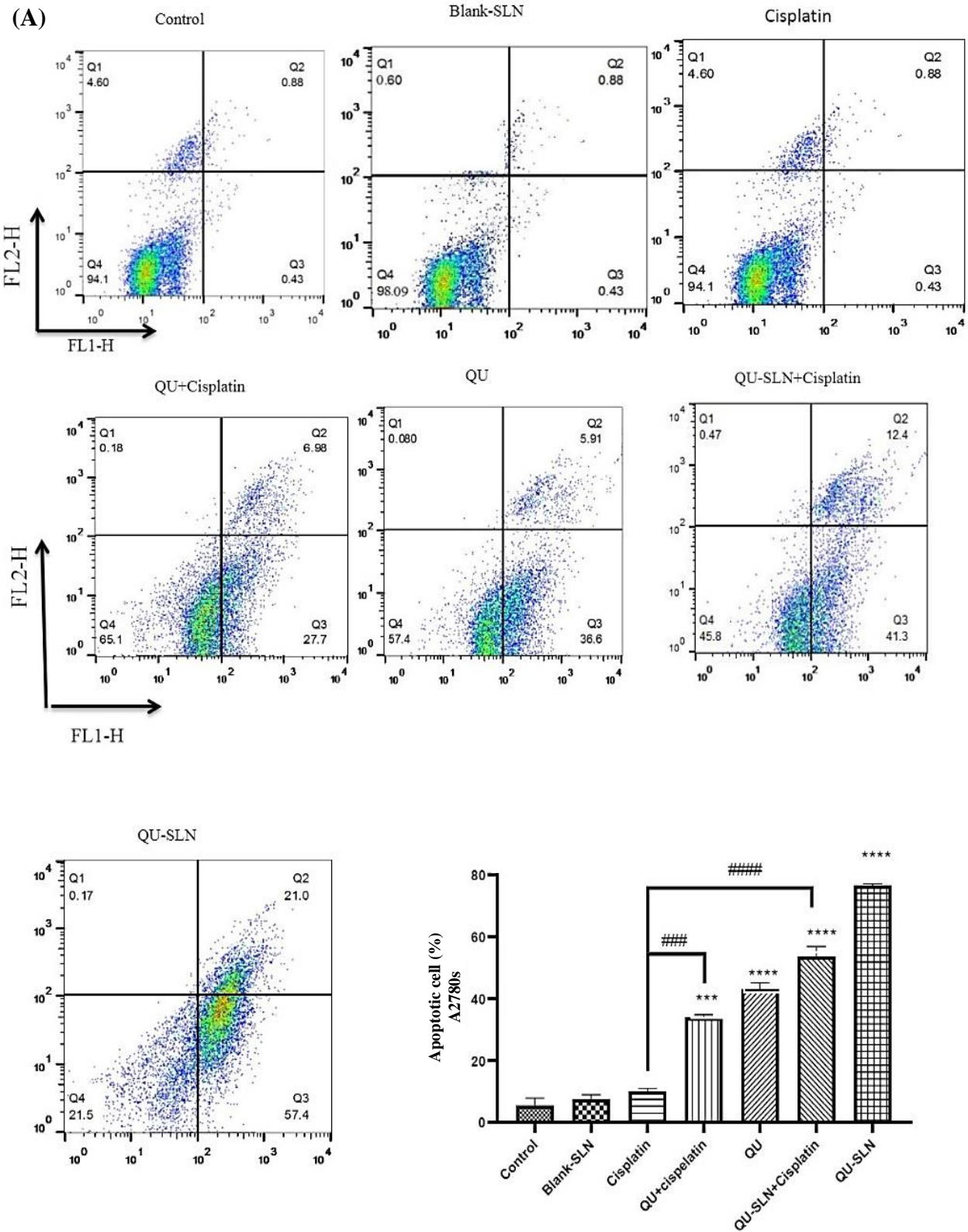
Wound healing assay

The wound healing assay assessed cell migration for 48 hours in both OC cell lines (Fig. 6A and 6B). Scratch assay images showed that all treatments resulted in the reduction in wound closure compared to the control. While the group treated with cisplatin showed an increased rate of cell migration, which was not statistically significant ($p > 0.05$; Fig. 6). However, the migration rate following treatment with QU-SLN in combination with cisplatin was significantly lower than those observed for cisplatin alone, blank-SLN, and the control groups. The migration studies revealed that SK-OV-3/DDP cells exhibited less motility than A2780s cells. Combining cisplatin with QU notably decreased wound closure rates in A2780s cells; however, it had less impact on SK-OV-3/DDP cells. The wound closure rates significantly reduced following treatment with QU-SLN in combination with cisplatin in both cell lines

at 24 and 48 hours ($p < 0.0001$; Fig. 6C and 6D). These results indicate that the combined treatment significantly decreases the motility of both SK-OV-3/DDP and A2780s cell lines. However, this effect is more remarkable in the sensitive OC cells than the resistant OC cells.

DISCUSSION

This work successfully incorporated QU into SLNs using a microemulsification process. The QU-SLN demonstrated excellent stability and a homogeneous size distribution. Additionally, the QU-SLNs showed a moderate rate of QU release, as indicated by the in vitro release profile. Due to the slow release of QU from the SLNs, medications should be administered gradually throughout the OC treatment.



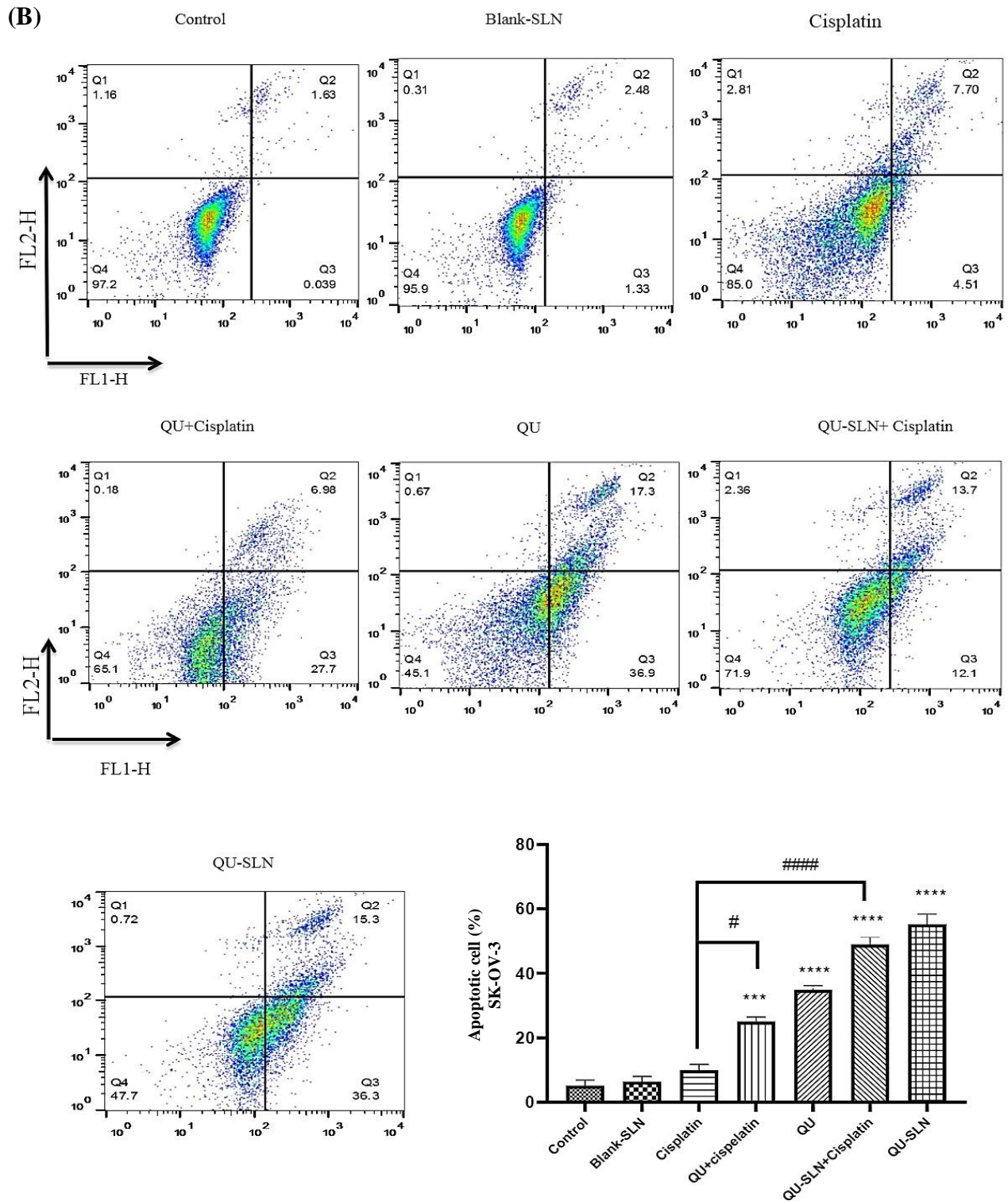


Fig 4. The dot plot charts from the flow cytometry analysis on A2780s (A) and SK-OV-3/DDP (B). The total apoptotic effect (early and late phases) in both treated and control groups is reflected in the quantitative data (A and B). In A2780s and SK-OV-3/DDP cells, the QU-SLN + cisplatin combination demonstrated the highest apoptotic rates. Blank-SLNs showed no apoptotic effect. The comparisons with the control group and the cisplatin 0.001 μ M group are shown by *** $p < 0.001$ and **** $p < 0.0001$ and # $p < 0.05$, ### $p < 0.001$, and #### $p < 0.0001$, respectively.

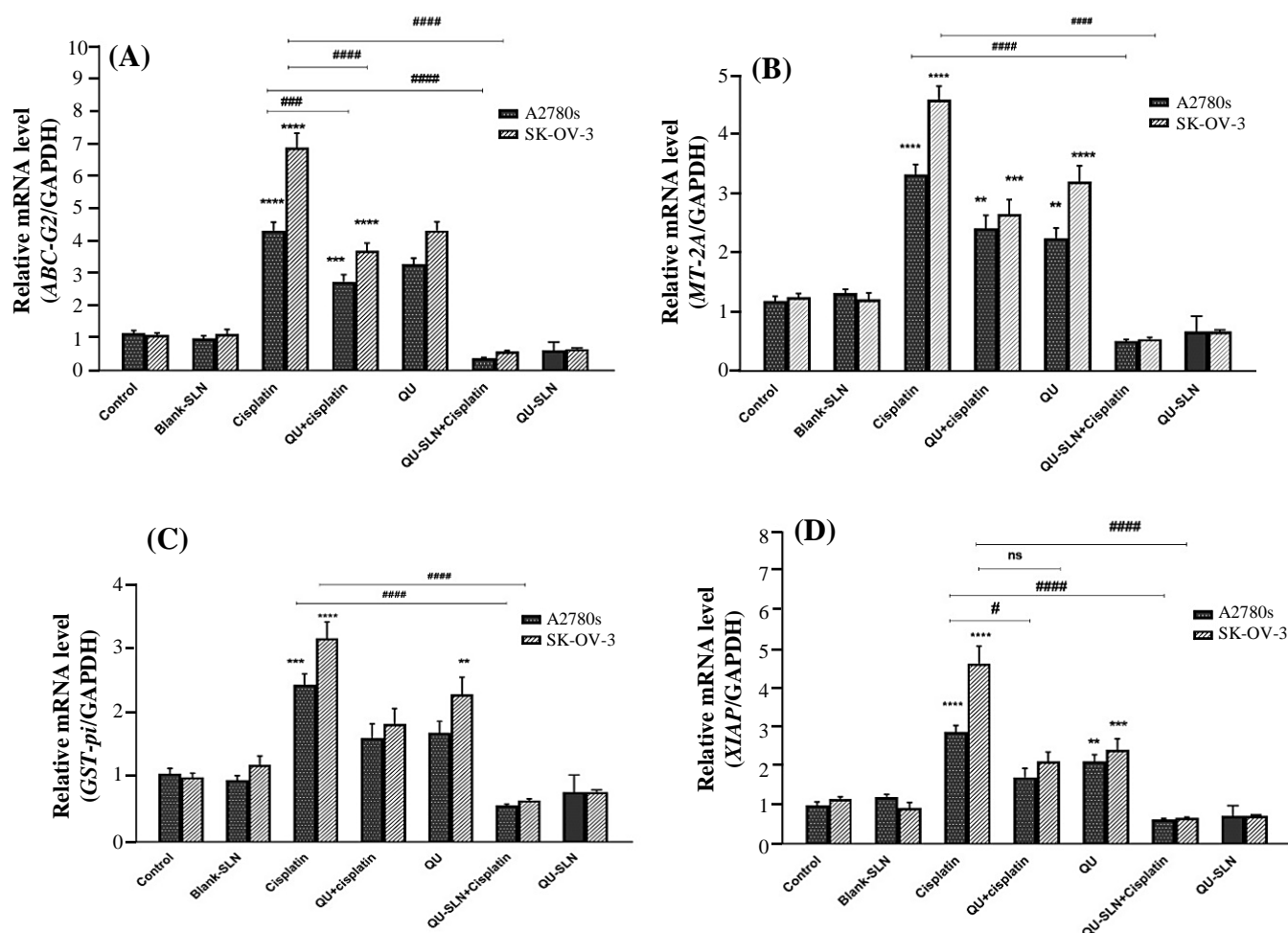


Fig. 5. Gene expression levels for *ABC-G2* (A), *MT-2A* (B), *GST-pi* (C), and *XIAP* (D) in A2780s and SK-OV-3/DDP cells. The illustration exhibits gene expression in the treated and untreated cells including Blank-SLN, cisplatin, QU + cisplatin, QU, QU-SLN + cisplatin, and QU-SLN. The data are shown as the mean \pm SD. Statistical significance when compared to the control group (* $p < 0.01$, ** $p < 0.001$, *** $p < 0.0001$); statistical significance when compared to the cisplatin 0.001 μM group (# $p < 0.05$, ### $p < 0.001$, #### $p < 0.0001$).

Many studies have demonstrated that SLNs are effective carriers for flavonoids and antitumor drugs. The findings have indicated that encapsulating curcumin and retinoic acid in SLNs significantly enhances their anticancer effect on OC cell lines^[16]. According to Jagdale et al., treatment with SLN-loaded anticancer drugs, including paclitaxel, yielded more desirable results in OC cells compared to drug treatment alone^[17]. Raut et al. have also demonstrated the efficacy of cisplatin loaded in SLNs^[18]. Wu et al. provided a brief summary of nanoparticle-based combination therapies, which primarily include combinations of anticancer drugs, gene therapy, and chemotherapy^[19], highlighting the benefits of treating OC with nanocarriers in combination. Our study found that encapsulating QU in SLNs significantly enhanced its antiproliferative effects in OC cells, likely due to the improved cellular penetration. Lu et al. linked this enhancement to the

increased solubility and stability of QU, which resulted in higher concentrations of the compound in MCF-7 cells^[20]. Additionally, Vijayakumar et al. demonstrated that SLNs markedly improved QU uptake in Caco-2 cells, leading to more uniform distribution compared to free QU in distilled water^[14].

Morphological analysis of the QU-SLN formulation utilizing TEM and DLS revealed average nanoparticle diameters of 150 ± 20.5 nm and 156 nm, respectively. This consistency indicates that nanoparticles smaller than 156 nm can help enhance cellular uptake, thereby improving the bioavailability and effectiveness of encapsulated QU. Further characterization through FTIR spectral analysis confirmed the successful formulation of QU-SLN, highlighting essential molecular interactions between QU and the solid lipid matrix that contributes to stability and efficacy of the formulation. The negative surface charge of -27.7 mV

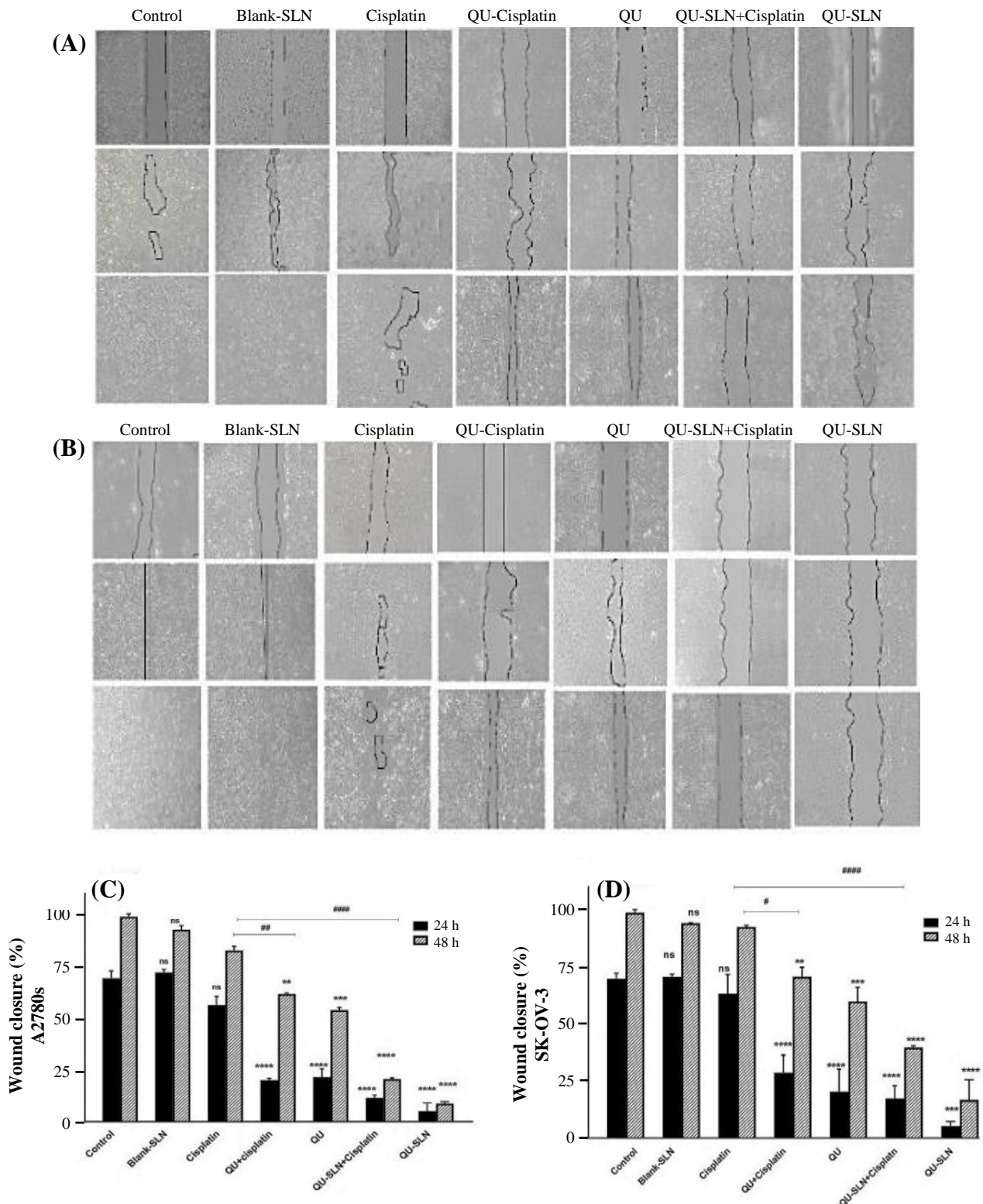


Fig. 6. The migration of (A) A2780s and (B) SK-OV-3 cells following 24 and 48 hours of treatment with blank-SLN, cisplatin, QU + cisplatin, QU, QU-SLN + cisplatin, and QU-SLN groups. The captured images showed the wound-healing process in both cell lines, untreated and treated with blank-SLN, QC, and QC-SLN over 24 and 48 hours (A and B). The wound area was quantified using ImageJ, and the values are presented as mean \pm SD (C and D). Statistically significant differences are denoted as follows: ** $p < 0.01$, **** $p < 0.0001$ when compared with the control group; # $p < 0.05$, ## $p < 0.01$, ### $p < 0.001$, #### $p < 0.0001$ when compared with the QC.

and a PDI of 0.50 ± 0.04 indicate favorable colloidal stability and predictable in vitro behavior. These results collectively highlight the potential of QU-SLNs to enhance both bioavailability of QU in managing OC. Similarly, Niazvand et al. reported a negative zeta potential ranging from -1.1 to -23.6 mV, with EEs between 67.6% and 98.9%. Their most effective formulation, quercetin-nanoparticle, exhibited a particle size of 85.5 ± 8.5 nm and a zeta potential of -22.5 ± 0.6 , with TEM images showing discrete, spherical nanoparticles^[21]. Herein, QU-SLN formulation demonstrated a remarkable EE of 99.6% and a drug loading of 1.81%. In comparison, the study by Talei et al. reported niosomal nanocarriers containing QU with an EE of 49%^[22]. Additionally, Lu, B reported niosomal nanocarriers containing QU with a drug entrapment efficiency of $87.3 \pm 1.6\%$ ^[23]. Thus, our formulation significantly outperforms these previous studies, showcasing a superior EE, which reflects the exceptional ability of SLNs to entrap and protect drug molecules, which is a crucial factor for the successful delivery of therapeutic agents.

Cisplatin exerts its anticancer effects by binding to DNA; however, its efficacy is often compromised by drug resistance, which is influenced by factors such as low solubility and protein binding^[24]. This resistance is particularly pronounced in solid tumors, where high interstitial fluid pressure limits drug penetration^[25]. Hence, the establishment of resistant OC cell lines is facilitated by exposure to low concentrations of the drug^[26,27]. Combining cisplatin with sensitizing agents presents a promising strategy to combat this resistance^[28]. Therefore, we developed a new QU-related drug, QU-SLN, for use on OC cells. This approach holds promise in overcoming the drug resistance commonly associated with chemotherapeutics like cisplatin by altering the pharmacokinetics and biodistribution of the drug.

The results of this study showed that the IC_{50} values of QU on the A2780s and SK-OV-3/DDP cells were 80 and 150 μ M, respectively, after 48 hours. The obtained IC_{50} value for the OC cells is similar to that reported by Catanzaro et al.^[29]. Although both A2780 and SK-OV-3/DDP cells had much lower IC_{50} values for QU, QU-SLNs demonstrated a more pronounced cytotoxic effect on them, as indicated by their respective IC_{50} values of 35.52 and 36.16 μ M. Our results indicated that cell survival exceeded 100% at a concentration of 1 μ M cisplatin in SK-OV-3/DDP cells, indicating resistance to cisplatin, as evidenced by the elevated IC_{50} values observed in this study.

Research has demonstrated that SK-OV-3/DDP cells develop TRAIL tolerance in response to 1 μ M of cisplatin, while higher concentrations (10 μ M) did not elicit the same effect. These findings elucidate the

mechanism behind cisplatin resistance observed in OC patients at low doses, suggesting that TRAIL tolerance may play a significant role in this phenomenon^[30]. Consistent with our results, Yi et al. have reported that QU increases the sensitivity of OC cells to TRAIL in response to a low concentration of cisplatin (1 μ M)^[31]. A prior study has demonstrated the suppressive influence of QU on the viability of these cells^[32].

The colony formation assay results revealed that treatment with QU combined with cisplatin reduced colony counts by 33.2% for A2780s cells and 32% for SK-OV-3/DDP cells compared to the cisplatin group. In contrast, combining QU-SLN and cisplatin significantly decreased colony counts by 71.2% in A2780s and 66% in SK-OV-3/DDP cells. These findings indicate that the efficacy of QU-SLN in conjunction with cisplatin is markedly enhanced compared to the QU and cisplatin combination. Our results are consistent with a previous study demonstrating a substantial decrease in colony numbers when QU is used alongside cisplatin, highlighting the potential of QU-SLNs to improve therapeutic outcomes in OC treatment^[33].

Two commonly used metrics for evaluating the efficacy of antitumor therapies are apoptosis and cell viability. Anticancer agents typically induce apoptosis in proliferating cells, leading to their elimination^[34]. The flow cytometry results in our study demonstrated that combining QU-SLN and cisplatin significantly increased the apoptosis rate, including both early and late stages, in A2780s and SK-OV-3/DDP cells compared to cisplatin group. Notably, the QU-SLN + cisplatin treatment induced a highly significant apoptosis, particularly in the A2780s cell line, which is more sensitive. However, it has previously reported that the QU + cisplatin combination induces necrosis in oral squamous cell carcinoma and OC cells^[35,36].

To investigate the underlying mechanisms of resistance to cisplatin, we evaluated the expression of four critical regulatory proteins associated with acquired cisplatin resistance: XIAP, GST-pi, ABC-G2, and MT-2A, as well as analyzed gene and mRNA expression levels. In both OC cell lines, exposure to 0.001 μ M cisplatin increased the mRNA level of XIAP, ABC-G2, MT-2A, and GST-pi. Notably, the combination of QU and cisplatin resulted in a reduction in the expression of these genes; however, this downregulation was more pronounced with QU-SLN combined with cisplatin, particularly in the more sensitive A2780s cell line. The mRNA expression in both cell lines significantly decreased with the QU-SLN + cisplatin treatment. These findings align with previous research by van Zanden et al. who demonstrated that QU can suppress GST-pi activity following QU exposure^[37]. In response to cisplatin and QU-SLN therapy, we observed a correlation between GST-pi and MT expression. While

our findings support these observations, Surowiak et al. highlighted a positive correlation between GST-pi expression at first-look laparotomies and MT expression in OC, suggesting that increased levels of both gene expression may promote resistance to cisplatin^[38]. Previously, Yang and colleagues have assessed the expression of NF-κB-dependent genes, including *COX-2*, *FLIP*, *Bcl-2*, *Bcl-xL*, and *XIAP* and demonstrated that these genes are associated with chemoresistance^[39]. In this context, the overexpression of *XIAP* has been observed in nearly 60 human cancer cell lines and across various cancer types, correlating with chemoresistance and poor prognosis^[40]. This observation underscores the importance of targeting GST-pi and MT in developing strategies to overcome resistance to platinum-based therapies.

In this study, we conducted a wound-healing assay to evaluate the impact of quality control on cell migration, a critical characteristic in OC progression. Our findings

indicated that treatment with QU combined with 0.001 μM of cisplatin significantly inhibited wound closure, demonstrating a reduction in cell migration, particularly in the A2780s and SK-OV-3/DDP cell lines at 48 h. These results are consistent with a previous investigation that has reported QU can effectively inhibit the migration of human metastatic OC (PA-1) cells in a dose-dependent manner. This finding suggests that QU significantly limits the migratory capabilities of metastatic OC cells^[41].

The present study explored a novel approach to the treatment of OC by reversing cisplatin resistance through combination therapy with QU and cisplatin. Using the SK-OV-3/DDP cell line, known for its resistance, alongside the sensitive A2780s line, the results demonstrated that QU-SLN combined with cisplatin exhibited a synergistic effect. This approach shows promise for overcoming resistance and improving therapeutic outcomes in OC (Fig. 7).

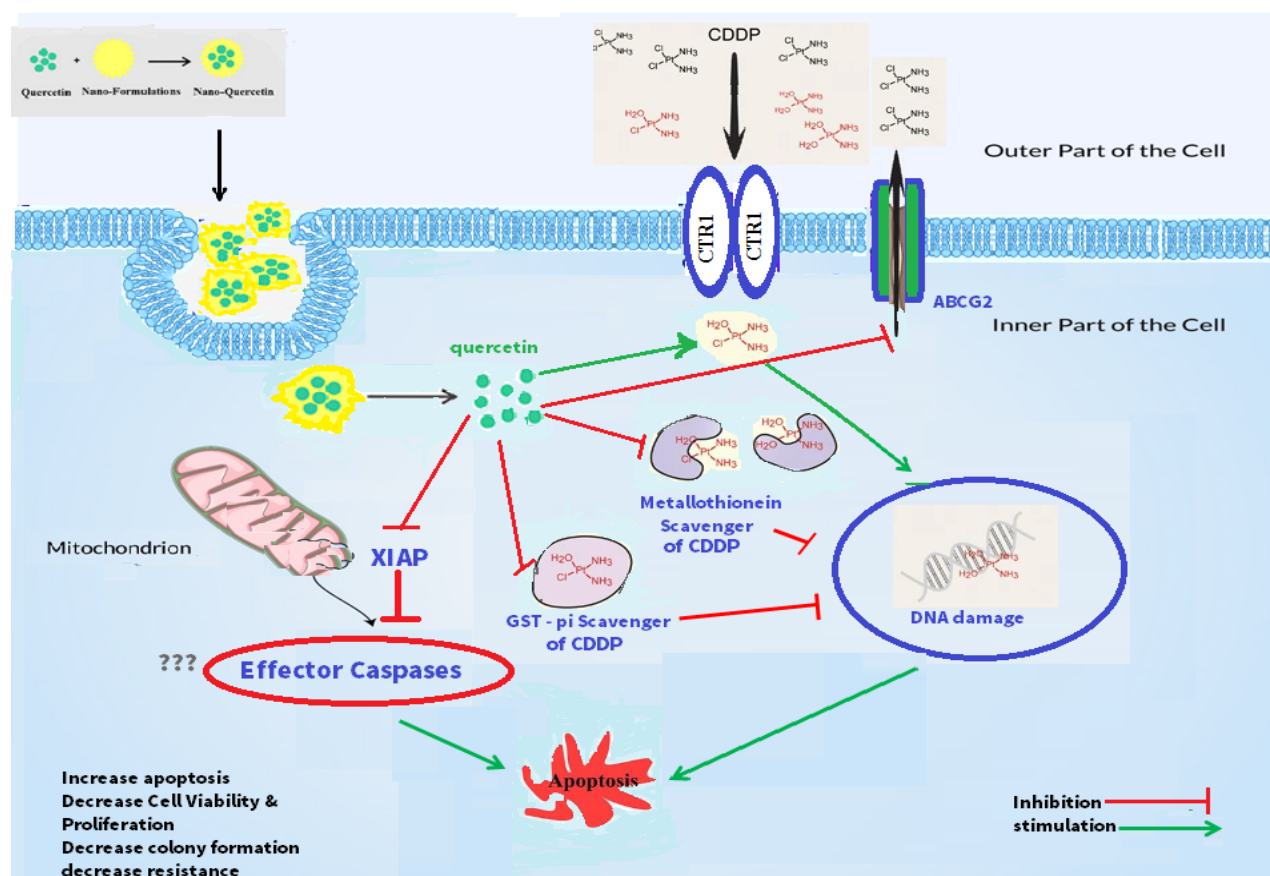


Fig. 7. The schematic diagram showing the mechanisms underlying cisplatin (CDDP) resistance in OC cells, particularly at a concentration of 0.001 μM. It highlights the suppression of critical genes associated with cisplatin resistance, specifically *XIAP*, *GST-pi*, *ABC-G2*, and *MT-2A*. Additionally, the treatment impairs the migratory potential of OC cells, which is a crucial factor contributing to resistance. This reduction in migration may facilitate the accumulation of cisplatin within the cells, leading to increased DNA damage and subsequent cell death.

CONCLUSION

This work presents a novel strategy for overcoming OC cisplatin resistance by encapsulating QU in SLNs. In addition to improving the effectiveness of cisplatin against resistant OC cell lines, SK-OV-3/DDP and A2780s, the QU-SLN formulation enhanced its bioavailability through controlled release mechanisms. This combination therapy significantly decreased cell viability and triggered apoptosis via the intrinsic apoptotic pathway, characterized by elevated caspase activation and mitochondrial dysfunction. Furthermore, QU-SLNs inhibited cancer cell migration while downregulating key genes associated with cisplatin resistance, including *XIAP*, *GST-pi*, *ABC-G2*, and *MT-2A*. These findings suggest that combining QU-SLNs with cisplatin may enhance treatment outcomes by increasing cellular sensitivity to apoptosis; however, additional clinical research is required to verify its safety and effectiveness.

DECLARATIONS

Acknowledgments

This research is derived from the thesis of Masoumeh Shamsi, with financial support provided by the Cellular and Molecular Research Centre at the Medical Basic Science Research Institute, Ahvaz Jundishapur University of Medical Sciences, Ahvaz, Iran. No artificial intelligence services were used for the preparation of this manuscript.

Ethical approval

All the experimental procedures in this study were approved by the Research Ethics Committee of Ahvaz Jundishapur University of Medical Sciences, Ahvaz, Iran (ethical code: IR.AJUMS.MEDICINE.REC.1400.010).

Consent to participate

Not applicable.

Consent for publication

All authors reviewed the results and approved the final version of the manuscript.

Authors' contributions

MS: contributed to data collection, interpretation, and analysis; HBR and AK: drafting and updating the material; MH: data analysis and interpretation; MR: conceived and designed the study.

Data availability

All data is provided in the manuscript and in additional files. All data are available on request.

Competing interests

The authors declare that they have no competing interests.

Funding

This work was funded by grant number CMRC-0020 from the Cellular and Molecular Research Center at the Medical Basic Sciences Research Institute of Ahvaz Jundishapur University of Medical Sciences, Ahvaz, Iran.

Supplementary information

The online version contains supplementary material.

REFERENCES

- Gao X, Wang B, Wei X, Men K, Zheng F, Zhou Y, et al. Anticancer effect and mechanism of polymer micelle-encapsulated quercetin on ovarian cancer. *Nanoscale*. 2012;4(22):7021-30.
- Gupta S, Pathak Y, Gupta MK, Vyas SP. Nanoscale drug delivery strategies for therapy of ovarian cancer: conventional vs targeted. *Artif Cells Nanomed Biotechnol*. 2019;47(1):4066-88.
- Hascicek C, Gun O. Nano drug delivery systems for ovarian cancer therapy. *Integr Cancer Sci Ther*. 2017;4:1-4.
- Momenimovahed Z, Tiznobaik A, Taheri S, Salehiniya H. Ovarian cancer in the world: epidemiology and risk factors. *Int J Womens Health*. 2019:287-99.
- Sheffield BS, Hwang HC, Lee AF, Thompson K, Rodriguez S, H Tse C, et al. BAP1 immunohistochemistry and p16 FISH to separate benign from malignant mesothelial proliferations. *Am J Surg Pathol*. 2015;39(7):977-82.
- Niu B, Liao K, Zhou Y, Wen T, Quan G, Pan X, et al. Application of glutathione depletion in cancer therapy: Enhanced ROS-based therapy, ferroptosis, and chemotherapy. *Biomaterials*. 2021;277:121110.
- Chen Y, Bieber MM, Teng NN. Hedgehog signaling regulates drug sensitivity by targeting ABC transporters ABCB1 and ABCG2 in epithelial ovarian cancer. *Mol Carcinog*. 2014;53(8):625-34.
- Shaw TJ, Lacasse EC, Durkin JP, Vanderhyden BC. Downregulation of XIAP expression in ovarian cancer cells induces cell death in vitro and in vivo. *Int J Cancer*. 2008;122(6):1430-4.
- Xie Y, Long Q, Wu Q, Shi S, Dai M, Liu Y, et al. Improving therapeutic effect in ovarian peritoneal carcinomatosis with honokiol nanoparticles in a thermosensitive hydrogel composite. *Rsc Adv*. 2012;2:7759-71
- Bahari LAS, Hamishehkar H. The impact of variables on particle size of solid lipid nanoparticles and

- nanostructured lipid carriers; a comparative literature review. *Adv Pharm Bull.* 2016;6(2):143-51.
11. Niazvand F, Orazizadeh M, Khorsandi L, Abbaspour M, Mansouri E, Khodadadi A. Effects of quercetin-loaded nanoparticles on MCF-7 human breast cancer cells. *Medicina.* 2019;55(4):114.
 12. Mishra V, Bansal KK, Verma A, Yadav N, Thakur S, Sudhakar K, et al. Solid lipid nanoparticles: Emerging colloidal nano drug delivery systems. *Pharmaceutics.* 2018;10(4):191.
 13. Ghasemiyeh P, Mohammadi-Samani S. Solid lipid nanoparticles and nanostructured lipid carriers as novel drug delivery systems: Applications, advantages and disadvantages. *Res Pharm Sci.* 2018;13(4):288-303.
 14. Vijayakumar A, Baskaran R, Jang YS, Oh SH, Yoo BK. Quercetin-loaded solid lipid nanoparticle dispersion with improved physicochemical properties and cellular uptake. *AAPS Pharm Sci Tech.* 2017;18(3):875-83.
 15. Qiu C, Zhang Z, Li X, Sang S, McClements DJ, Chen L, et al. Co-encapsulation of curcumin and quercetin with zein/HP- β -CD conjugates to enhance environmental resistance and antioxidant activity. *NPJ Sci Food.* 2023;7(1):29.
 16. Akanda M, Mithu MSH, Douroumis D. Solid lipid nanoparticles: An effective lipid-based technology for cancer treatment. *J Drug Deliv Sci Technol.* 2023;86(4):1-14.
 17. Jagdale S, Narwade M, Sheikh A, Md S, Salve R, Gajbhiye V, et al. GLUT1 transporter-facilitated solid lipid nanoparticles loaded with anti-cancer therapeutics for ovarian cancer targeting. *Int J Pharm.* 2023;637:122894.
 18. Raut ID, Doijad RC, Mohite SK, Manjappa AS. Preparation and characterization of solid lipid nanoparticles loaded with cisplatin. *J Drug Deliv Therapeut.* 2018;8(6):125-31.
 19. Wu Y, Yang Y, Lv X, Gao M, Gong X, Yao Q, et al. Nanoparticle-based combination therapy for ovarian cancer. *Int J Nanomedicine.* 2023;18:1965-87.
 20. Lu J, Sun D, Gao S, Gao Y, Ye J, Liu P. Cyclovirobuxine D induces autophagy-associated cell death via the Akt/mTOR pathway in MCF-7 human breast cancer cells. *J Pharmacol Sci.* 2014;125(1):74-82.
 21. Niazvand F, Khorsandi LS, Absalan F, Ashtari A. Effect of quercetin solid lipid nanoparticles on autophagy and Atg5 protein expression levels in human breast cancer cell line (MCF-7). *Yafteh.* 2020;22(2):144-59.
 22. Talei N, Daneshmand F, Mirhoseini M, Majdzadeh M, Haghirsadat BF. Fabrication and characterization of physicochemical niosomal nanocarriers containing quercetin flavonoids for therapeutic purposes. 2020;15(1):32-40.
 23. Lu B, Huang Y, Chen Z, Ye J, Xu H, Chen W, et al. Niosomal nanocarriers for enhanced skin delivery of quercetin with functions of anti-tyrosinase and antioxidant. *Molecules.* 2019;24(12):2322.
 24. Zamble DB. The responses of cellular proteins to cisplatin-damaged DNA. MIT Libraries. 1999:73344.
 25. Nagai N, Okuda R, Kinoshita M, Ogata H. Decomposition kinetics of cisplatin in human biological fluids. *J Pharm Pharmacol.* 1996;48(9):918-24.
 26. Li X, Ling V, Li PC. Same-single-cell analysis for the study of drug efflux modulation of multidrug resistant cells using a microfluidic chip. *Anal Chem.* 2008;80(11):4095-102.
 27. Petrović M, Todorović D. Biochemical and molecular mechanisms of action of cisplatin in cancer cells. *Med Biol.* 2016;18(1):12-18.
 28. Nessa MU, Beale P, Chan C, Yu JQ, Huq F. Synergism from combinations of cisplatin and oxaliplatin with quercetin and thymoquinone in human ovarian tumour models. *Anticancer Res.* 2011;31(11):3789-97.
 29. Catanzaro D, Ragazzi E, Vianello C, Caparotta L, Montopoli M. Effect of quercetin on cell cycle and cyclin expression in ovarian carcinoma and osteosarcoma cell lines. *Nat Prod Commun.* 2015;10(8):1365-8.
 30. Lu J, Zhang L, Xie F, Zhu L, Li X, Ouyang J, et al. Mild oxidative stress induced by a low dose of cisplatin contributes to the escape of TRAIL-mediated apoptosis in the ovarian cancer SKOV3 cell line. *Oncol Rep.* 2016;35(6):3427-34.
 31. Yi L, Zongyuan Y, Cheng G, Lingyun Z, GuiLian Y, Wei G. Quercetin enhances apoptotic effect of tumor necrosis factor-related apoptosis-inducing ligand (TRAIL) in ovarian cancer cells through reactive oxygen species (ROS) mediated CCAAT enhancer-binding protein homologous protein (CHOP)-death receptor 5 pathway. *Cancer Sci.* 2014;105(5):520-7.
 32. Ren M-X, Deng X-H, Ai F, Yuan G-Y, Song H-Y. Effect of quercetin on the proliferation of the human ovarian cancer cell line SKOV-3 in vitro. *Exp Ther Med.* 2015;10(2):579-83.
 33. Zhou J, Gong J, Ding C, Chen G. Quercetin induces the apoptosis of human ovarian carcinoma cells by upregulating the expression of microRNA-145. *Mol Med Rep.* 2015;12(2):3127-31.
 34. Scambia G, Ranelletti F, Panici PB, Piantelli M, Bonanno G, De Vincenzo R, et al. Inhibitory effect of quercetin on primary ovarian and endometrial cancers and synergistic activity with cis-diamminedichloroplatinum (II). *Gynecol Oncol.* 1992;45(1):13-9.
 35. Gordon JL, Brown MA, Reynolds MM. Cell-based methods for determination of efficacy for candidate therapeutics in the clinical management of cancer. *Diseases.* 2018;6(4):85.
 36. Li X, Guo S, Xiong X-K, Peng B-Y, Huang J-M, Chen M-F, et al. Combination of quercetin and cisplatin enhances apoptosis in OSCC cells by downregulating xIAP through the NF- κ B pathway. *J Cancer.* 2019;10(19):4509-21.
 37. Van Zanden JJ, Hamman OB, Van Iersel ML, Boeren S, Cnubben NH, Bello ML, et al. Inhibition of human glutathione S-transferase P1-1 by the flavonoid quercetin. *Chem Biol Interact.* 2003;145(2):139-48.
 38. Surowiak P, Materna V, Kaplenko I, Spaczyński M, Dietel M, Lage H, et al. Augmented expression of metallothionein and glutathione S-transferase pi as unfavourable prognostic factors in cisplatin-treated

- ovarian cancer patients. *Virchows Arch.* 2005;447(3):626-33.
39. Yang Y-I, Lee K-T, Park H-J, Kim TJ, Choi YS, Shih I-M, et al. Tectorigenin sensitizes paclitaxel-resistant human ovarian cancer cells through downregulation of the Akt and NF κ B pathway. *Carcinogenesis.* 2012;33(12):2488-98..
40. Miyamoto M, Takano M, Iwaya K, Shinomiya N, Kato M, Aoyama T, et al. X-chromosome-linked inhibitor of apoptosis as a key factor for chemoresistance in clear cell carcinoma of the ovary. *Br J Cancer.* 2014;110(12):2881-6.
41. Dhanaraj T, Mohan M, Arunakaran J. Quercetin attenuates metastatic ability of human metastatic ovarian cancer cells via modulating multiple signaling molecules involved in cell survival, proliferation, migration and adhesion. *Arch Biochem Biophys.* 2021;701:108795.